Crystal Structures of Fully La^{3+}-Exchanged Zeolite X: an Intrazeolitic La_2O_3 Continuum, Hexagonal Planar and Trigonally Monocapped Trigonal Prismatic Coordination

Hyun Sook Park and Karl Seff*

Department of Chemistry, University of Hawaii, Honolulu, Hawaii 96822

Received: June 25, 1999; In Final Form: September 22, 1999

Three single crystals of sodium zeolite X were fully La^{3+}-exchanged at 90 °C from aqueous solution (pH = 7.45, 7.45, and 6.89 at 22 °C, respectively). One was vacuum dehydrated at 400 °C (crystal 1), another at 22 °C (crystal 2), and the third remained fully hydrated (crystal 3). Their structures at 22 °C were determined by single-crystal X-ray crystallography in the cubic space groups $Fd\bar{3}m$ (a = 24.999(4) and 25.059(4) Å) and $Fd\bar{3}$ (a = 25.154 (3) Å), respectively. They were refined to the final error indices R_1 = 0.076, 0.091, and 0.078 with 471, 374, and 725 reflections, respectively, for which $F_o > 4\sigma(F_o)$. The number of La^{3+}, H_3O^+, and OH^- ions found in the three structures are about 38, 0, 18; 38, 28, 50; and 33, 16, 24, respectively, per unit cell. Crystal 1 also has 48 nonframework oxide ions and 92 H^+ ions per unit cell. In all cases overexchange occurred. In **crystal 1**, 32 La^{3+} ions per unit cell fill site I′, with the remaining six at 12-ring centers (site V). Each of these six coordinates to three OH^- ions and three water molecules in a near hexagonal planar manner. A tetrahedron of four La^{3+} ions at site I′ is found in each sodalite unit; each La^{3+} coordinates to three framework oxygens. This tetrahedron is interpenetrated by a tetrahedron of four oxide ions to give a distorted $La_4O_4^{4+}$ cube. These cubes are linked by oxide ions at site I to form a neutral La_2O_3 continuum; a binary intrazeolitic continuum had not been previously reported. In **crystal 2**, 28 La^{3+} ions are at site I′, eight at site V, and two at supercage centers (site IV). Four H_3O^+ ions are at site I′, 12 at site III′, and 12 at site II. In all, 64 water molecules per unit cell coordinate to La^{3+} ions or bridge between hydrated La^{3+} ions. Half of the sodalite units contain complete $La_4(OH)_4^{8+}$ "cubes", and the other half contain $La_3(OH)(OH_2)_3^{8+}$ units. Two of the eight supercages per unit cell are filled with large clusters. Each consists of a La^{3+} ion at its center (site IV), four La^{3+} ions near site V, six H_3O^+ ions, 19 water molecules, and 15 OH^- ions. In **crystal 3**, eight La^{3+} ions are at site I′, 24 at site II, and one at site V. Each sodalite unit contains a La^{3+} ion at site I′; this ion coordinates to three framework oxygens and to three OH^- ions. Each OH^- ion bridges to a La^{3+} ion at site II, and each triplet of OH^- ions is capped by a H_3O^+ ion. Each supercage contains three La^{3+} ions at site II and 19 water molecules. For the first time, the coordination geometries hexagonal planar (crystals 1 and 2) and trigonally monocapped trigonal-prismatic (crystal 3) are seen.

Introduction

Acid zeolites are of interest because of their catalytic properties.[1] Because of cation hydrolysis, rare earth ion-exchanged zeolites X and Y are highly acidic.[2−4] They also have enhanced hydrothermal stability; this is attributed to the oxide hydroxide rare earth clusters that form in sodalite units upon dehydration. Most lanthanum produced, "over 10^7 lbs/year as lanthanum rare-earth chloride, is used for molecular sieve catalysts for cracking crude petroleum."[5]

La_2O_3 doped with 0.5 mol % Yb^{3+} exhibits a sharp emission line whose energy is the sum of the energies of two single-ion transitions from an excited state to the ground state.[6] This luminescence is the result of a relatively strong interaction between the 4f electrons of the excited Yb^{3+} ions in the La_2O_3 host lattice.

Rare earth oxides become proton conductors upon exposure to atmospheres containing water vapor or other hydrogen-containing gases.[7] La_2O_3 doped with divalent cations such as Ca^{2+} [7] or Sr^{2+} [8] is a good oxygen ion conductor[9] and is a useful catalyst for the oxidative coupling of methane to form higher hydrocarbons.[10]

Olson et al.[11] prepared La^{3+}-exchanged zeolite X with unit cell composition $(La_2O_3)_{14.55}(Na_2O)_{0.2}(Al_2O_3)_{43.4}(SiO_2)_{105.1}$-$(H_2O)_{270}$ by batch exchange with aqueous $La(NO_3)_3$ (concentration and pH not given) at 100 °C for 13 days. In a hydrated crystal, 33 La^{3+} ions were found crystallographically per unit cell at three sites: I′, II, and V; about half of the lanthanum ions occupy site II. In the structure of a single crystal vacuum dehydrated at 350 °C, 30 La^{3+} ions per unit cell are equivalent at site I′.[11] These La^{3+} ions are μ_3-coordinated by nonframework oxygens.

Bennett and Smith's[12,13] results differ from Olson's.[11] They exchanged single crystals of faujasite (composition not given) with $La(NO_3)_3$ (concentration and pH not given) by batch methods at 95 °C for 16 days. One was then vacuum dehydrated at 475 °C for more than 4 days, followed by further evacuation at 775 °C. A second crystal was dehydrated at 420 °C in a nitrogen stream. Both crystal structures showed that most La^{3+} ions occupy site I and that sites I′ and II are sparsely occupied. They attribute the differences between their La^{3+} positions and those of Olson et al.[11] to the differing ion-exchange and dehydration conditions.[12] Hydronium ions from the hydrolysis of aqueous La^{3+} may have entered the zeolite during ion exchange and, after decomposition and possibly loss of H^+ with

* To whom correspondence should be addressed. E-mail: kseff@gold.chem.hawaii.edu.

10.1021/jp992153i CCC: $19.00
Published on Web 02/17/2000

framework oxygen as water during dehydration, may still be influencing the final La^{3+} positions. Finally, they reported that the La^{3+} ion distribution depended little on the dehydration temperature; it was nearly the same after dehydration at ambient temperature and at 420 °C.[13]

Scherzer et al. prepared La^{3+}-exchanged zeolite Y powder by ion exchange (1) with 10 wt % aqueous ammonium sulfate followed by (2) varying amounts of aqueous $LaCl_3$ whose pH was adjusted to 3.5 with dilute HCl.[14] Three samples were prepared: 24%, 53%, and 98% La^{3+}-exchanged zeolite Y. X-ray powder diffraction experiments showed that most of the La^{3+} ions in these freshly exchanged La,Na−Y zeolites occupy supercage positions after vacuum dehydration at room temperature. Each of the three samples was further divided into three portions which were treated as follows: (a) vacuum dehydration at 540 °C for 3 h, (b) steam treatment at 540 °C for 3 h, and (c) steam treatment at 820 °C for 3 h. This caused all La^{3+} ions in the 24% and 53% exchanged samples treated at 540 °C (a and b) to move to site I′. Only about 75% of the La^{3+} ions were at site I′ in the vacuum-dehydrated 98% La^{3+}-exchanged sample (a); the remainder are at site II.

An increase in steam treatment temperature from 540 to 820 °C enhances the dealumination process.[14] (Steam treatment of even NH_4−Y leads to a partially dealuminated framework.) Besides steam and temperature, the degree of dealumination depends on framework composition. It also depends on the extent of La^{3+} exchange. After steam treatment at 540 °C, 24% exchanged La−Y is the most dealuminated and 98% exchanged La−Y the least. The extent of dealumination was seen in the infrared spectra of 24% exchanged La−Y; the T−O asymmetric stretching band shifts from 1034 cm^{-1} (540 °C, vacuum) to 1045 cm^{-1} (540 °C, steam) to 1075 cm^{-1} (820 °C, steam), indicating increasing dealumination (increasing Si content in the zeolite framework).

Nery et al.[15] prepared La^{3+}-exchanged zeolite Y powder (composition not given) by ion exchange (1) with 5% aqueous ammonium sulfate followed by (2) freshly prepared aqueous $LaCl_3$ solution (concentration and pH not given) in a stirred vessel.[16] One sample of La,Na−Y was dried overnight at 120 °C (LaNaY). A second sample was vacuum dehydrated (calcined) at 500 °C for 1 h (LaNaYc). A third sample was prepared by steam treatment at 500 °C for 1 h (LaNaYs). The crystal structures were determined by the Rietveld method. In LaNaY, 0.8 and 5.0 La^{3+} ions were found at sites II and V, respectively, and 20.2 Na^+ ions were found at site I′. More La^{3+} ions were found in LaNaYc and LaNaYs; site I′ is occupied by about 10.4 La^{3+} ions in both. In addition, 9.8 Al^{3+} ions were found at site I′ and 20 Na^+ ions at site II in both LaNaYc and LaNaYs. Dealumination upon dehydration of rare earth exchanged zeolite Y is likely to result from attack by the protons produced by rare earth cation hydrolysis.[14−18]

Infrared absorption studies by Rabo et al. of Ce^{3+}- and Ca^{2+}-exchanged zeolite Y show strong Ce−OH and Ca−OH bands upon vacuum dehydration at 500 °C.[19] These bands disappear when this is repeated at 700 °C, indicating the completion of the dehydration process (removal of all hydrogens as water: removal of H_2O and OH^-/H^+ pairs including those in hydroxyl groups ($2\ -OH^- \rightarrow -O^{2-} + H_2O$)).

Experimental Section

1. Crystal Preparation. Large single crystals of Na−X, stoichiometry $Na_{92}Si_{100}Al_{92}O_{384}$ per unit cell, were prepared in Leningrad, now St. Petersburg, Russia.[20] Three colorless octahedral single crystals about 0.13 mm in cross section were selected. Each was lodged in a fine Pyrex capillary. Ion exchanges were accomplished by allowing 0.033 M aqueous $La(C_2H_3O_2)_3$ (Strem, 99.9% $La(C_2H_3O_2)_3$, Ca < 70 ppm, Y < 15 ppm, Si < 10 ppm, Al < 10 ppm, Pb < 7 ppm, Cu < 3 ppm, Fe < 3 ppm, Mg < 3 ppm, Yb < 3 ppm, and Er < 2 ppm; pH = 7.45, 7.45, and 6.89, respectively, at 22 °C) to flow past the crystals for 6 to 8 days at 90 °C. During these processes, the flow stopped several times due to blockage by a milky white precipitate. Each time the crystal was transferred to a new capillary and the ion exchange flow was resumed.

After ion exchange of the first crystal, the capillary containing the crystal was attached to a vacuum system and the crystal temperature was slowly increased by ca. 15 °C/h until it reached 400 °C with $P = 1 \times 10^{-5}$ Torr for 48 h. While these conditions were maintained, the hot contiguous downstream lengths of the vacuum system, including a sequential U-tube of beads of zeolite 5A fully activated in situ, were cooled to ambient temperature to prevent the movement of water molecules from more distant parts of the vacuum system to the crystal. Only then was the crystal, still under vacuum in its capillary, allowed to cool to room temperature. It was sealed in its capillary and removed from the vacuum line by torch. Under the microscope, it appeared very pale red−brown; trace oxides of Pb, Cu, Fe, and/or Er could be responsible. The second crystal was vacuum dehydrated at $P = 2 \times 10^{-5}$ Torr and $T = 21$ °C for 2 days before being sealed in its capillary by torch. The capillary containing the third crystal was sealed at one end by torch, a very small amount of water was added, and the capillary was then sealed at the other end with epoxy glue.

2. Microprobe Analysis. Spectrometer scans were done on a Cameca SX50 electron microprobe. The operating conditions were 15 kV and 15 nA. A hydrated crystal La^{3+}-exchanged as above was placed on a conductive carbon tape using epoxy glue without coating. The depth of analysis was a few micrometers, about 1000 unit cells. Large $^1La(L\alpha)$ peaks were observed as expected. No significant residual sodium content was seen. There is no evidence for a composition change in the zeolite framework due to ion exchange; both $^1Si(K\alpha)$ and $^1Al(K\alpha)$ peaks were strong.

3. X-ray Diffraction and Data Collection. Diffraction data were collected with an automated Siemens P3 four-circle computer-controlled diffractometer equipped with a pulse-height analyzer and a graphite monochromator. The $\theta-2\theta$ scan technique was used for data collection. The intensities of all lattice points for which $3° < 2\theta < 50°$ were scanned at a constant rate of 3.0° min^{-1} from 1.0° below the $K\alpha_1$ peak to 1.0° above the $K\alpha_2$ maximum. Background intensity was counted at each end of a scan range for a time equal to one-half the scan time. The intensities of three reflections in diverse regions of reciprocal space were recorded every 97 reflections to monitor crystal and instrument stability; only insignificant fluctuations about mean intensities were seen. Lorentz, polarization, and profile corrections were made. Absorption corrections, made empirically using a ψ scan, had a negligible effect on the data because the crystals were isotropic in shape.

The reflection conditions (hkl: $h + k$, $k + l$, $l + h = 2n$; $0kl$: $k + l = 4n$) indicate that the space group is either $Fd\bar{3}$ or $Fd\bar{3}m$. $Fd\bar{3}$ was initially chosen for all three crystals because most crystals from this synthesis batch, regardless of subsequent chemical treatment, have been refined successfully in $Fd\bar{3}$.[21] Their diffraction data refines to error indices lower in $Fd\bar{3}$ than in $Fd\bar{3}m$, with mean Al−O distances correctly ca. 0.10(3) Å longer than mean Si−O distances.[21] This is in agreement with Loewenstein's rule[22] which requires alternation of Si and Al

atoms for crystals with Si/Al = 1, and requires that also, at least in the short range, for these crystals whose Si/Al ratio is 1.09. An inspection of the diffraction intensity data from these crystals generally shows some strong intensity inequalities for *hkl* and *khl* reflections, indicating the absence of the mirror plane of $Fd\bar{3}m$, hence $Fd\bar{3}$.

For crystals 1 and 2, however, $Fd\bar{3}$ was rejected and the space group $Fd\bar{3}m$ was used. In least-squares refinement only a negligible difference (ca. 0.003 Å) was seen between the mean Al−O and Si−O bond lengths, and no increases in error indices were seen when the space group was changed to $Fd\bar{3}m$. The erasure of the ca. 0.10 Å difference between Al−O and Si−O indicates that the Si,Al composition at the Si position is essentially the same as that at the Al position, and therefore the same as that of the entire crystal; the long-range Si,Al ordering has been lost. This can occur most easily by the establishment of antidomain structure.[23] Intrazeolitic acidity, including that resulting from cations such as Ni^{2+} and Co^{2+} which hydrolyze strongly within the zeolite, appears to be responsible for the loss of long-range order.[21] The loss of small to moderate amounts of Al from the zeolite framework can lead readily to the formation of antidomains.[21] La^{3+} is hydrolyzing very strongly in these structures.

The cubic space group $Fd\bar{3}$ could, however, be used for crystal 3. It was justified (a) by the reflection conditions given above, (b) by intensity inequalities observed for *hkl* and *khl* reflections, and (c) by numerous previous determinations using crystals from the same batch that had been subjected to relatively mild chemical treatment. This space group requires that the Si and Al atoms alternate in obeyance of Loewenstein's rule;[22] the compositional deviation of Si/Al from 1 could be accommodated if about 4% of the Al sites are occupied by Si atoms.[23] However, the mean Si−O and Al−O distances (vide infra) indicate by their closeness that the long-range order in this crystal is compromised, presumeably for the same reasons that it was lost in crystals 1 and 2.

All unit cell constants at 21 °C, determined by least-squares refinement of selected intense reflections, are given in Table 1 together with other data describing the diffraction work.

TABLE 1: Summary of Experimental Data

	crystal number		
	1	2	3
crystal cross section (mm)	0.135	0.130	0.130
ion exchange T (°C)	90	90	90
ion exchange t (days)	6	6	8
pH of exchange soln at 22 °C	7.45	7.45	6.89
desolvation T (°C)	400	22	-
T (°C) in data collection	21	21	21
scan technique	θ-2θ	θ-2θ	θ-2θ
radiation (Mo $K\alpha$) λ_1 (Å)	0.70930	0.70930	0.70930
λ_2 (Å)	0.71359	0.71359	0.71359
unit cell constant, a (Å)	24.999(4)	25.059(4)	25.154(3)
2θ range for a (deg)	10.6−18.7	10.6−18.7	10.6−18.7
no. of reflections for a	35	27	16
space group	$Fd\bar{3}m$	$Fd\bar{3}m$	$Fd\bar{3}$
2θ range, data collection (deg)	3−55	3−50	3−50
no. of reflections gathered	4815	3881	3757
no. of unique reflections, n	907	716	1179
no. with $F_o > 4\sigma(F_o)$	471	374	725
no. of parameters, s	47	60	98
data/parameter ratio, n/s	19.3	19.6	12.0
merging R (all intensities)	0.205	0.189	0.179
weighting parameters, a/b[a]	0.1237/0.0	0.1335/0.0	0.0980/0.0
R_1 (using $F_o > 4\sigma(F_o)$)[b]	0.076	0.091	0.077
wR_2 (using all intensities)[c]	0.234	0.250	0.220
goodness of fit[d]	0.937	1.125	1.084
μ (mm^{-1})	2.57	2.55	2.52
ρ_{cal} (Mg/m^3)	1.77	1.75	1.73

[a] Weighting parameters = $1/\{\sigma^2(F_o^2) + (aP)^2 + bP\}$, where $P = [\mathrm{Max}(F_o^2, 0) + 2F_c^2]/3$. [b] $R_1 = \sum|F_o - |F_c||/\sum F_o$ (based on F) is calculated using only those reflections for which $F_o > 4\sigma(F_o)$. [c] $wR_2 = \{\sum w(F_o^2 - F_c^2)^2/\sum w(F_o^2)^2\}^{1/2}$ (based on F^2) is calculated using all intensities. [d] Goodness of fit = $\{\sum w(F_o^2 - F_c^2)^2/(n - s)\}^{1/2}$.

Structure Determination

All least-squares refinements[24] were full-matrix and were done on F^2 using all unique reflections without an $n\sigma$ cutoff. This work has attempted to provide as complete a description of the structures as possible, given the limited amount of data, the disorder within the framework, and the many positions of partial occupancy, often overlapping. The results may be in error in some details.

1. Crystal 1 (Vacuum Dehydrated at 400 °C). Least-squares refinement was initiated with the atomic positions of the framework atoms [(Si,Al), O(1), O(2), O(3), and O(4)] in the structure of fully dehydrated, partially Cu^{2+}-exchanged zeolite Y.[26] Because the SiO_4 and AlO_4 tetrahedra are indistinguishable in the space group $Fd\bar{3}m$, only the average species, (Si,Al), is considered in this work.

Isotropic refinement of the framework atoms yielded the error indices $R_1 = 0.60$ and $wR_2 = 0.89$ (definitions in footnotes to Table 1). The initial Fourier electron density difference function revealed two large peaks at (0.068, 0.068, 0.068) and (0.500, 0.500, 0.500). Isotropic refinement including these peaks as La(I′) and La(V) converged with $R_1 = 0.13$ and $wR_2 = 0.36$.

A major peak was found at (0.165, 0.165, 0.165), O(6), on a subsequent Fourier function. Isotropic refinement including this peak converged with $R_1 = 0.11$ and $wR_2 = 0.29$. Similarly, another peak appeared at (0.0, 0.0, 0.0), O(7). This refinement converged with $R_1 = 0.096$ and $wR_2 = 0.27$.

Anisotropic refinement of framework atoms and La(I′), O(6), and O(7) converged with $R_1 = 0.088$ and $wR_2 = 0.26$. Because the occupancies at La(I′), O(6), and O(7) were approximately at their maximum values, they were fixed at these full values. Refinement converged with $R_1 = 0.087$ and $wR_2 = 0.26$.

Isotropic refinement of a peak at (0.200, 0.200, 0.431), O(5), from a subsequent difference Fourier function converged with $R_1 = 0.081$ and $wR_2 = 0.25$. Allowing La(V) to refine anisotropically led to $R_1 = 0.076$ and $wR_2 = 0.222$. It was observed that the occupancies at La(V) and O(5) were refining in the ratio of 1:6; introducing this as a constraint did not affect the R values. The goodness-of-fit is 0.94 (see Table 1). The largest peaks on the final difference Fourier function were all impossibly close to other atoms. The final refinement with the final recommended value of a in the weighting scheme (see Table 1) converged with $R_1 = 0.076$ and $wR_2 = 0.23$. The final structural parameters and selected interatomic distances and angles are presented in Tables 2a and 3, respectively.

Atomic form factors for Si, O, and La were used for this and the two subsequent structures.[25] The form factor for (Si,Al) in crystals 1 and 2 was that of Si diminished by a factor of 0.966 to give the correct number of electrons at the Si/Al position.

2. Crystal 2 (Vacuum Dehydrated at 22 °C). Full-matrix least-squares refinement[24] was initiated with the same framework atomic positions as for crystal 1.[26] As above, only the average (Si,Al) position could be determined in this work. Isotropic refinement of the framework atoms yielded $R_1 = 0.58$ and $wR_2 = 0.88$. A difference Fourier function revealed two large peaks at (0.067, 0.067, 0.067) and (0.165, 0.165, 0.165). Isotropic refinement including these peaks as La(I′) and O(6) converged with $R_1 = 0.16$ and $wR_2 = 0.43$.

TABLE 2: Positional,[a] Thermal,[b] and Occupancy Parameters

atom	Wyckoff pos.	site	*x*	*y*	*z*	U_{11}[c] or U_{iso}	U_{22}	U_{33}	U_{23}	U_{13}	U_{12}	occupancy[d] varied	occupancy[d] fixed
						(a) Crystal 1							
Si	192(i)		−5449(12)	3619(11)	12693(13)	16(1)	16(1)	17(1)	−5(1)	−2(1)	2(1)		192
O(1)	96(g)		−10535(33)	10535(33)	0	25(4)	25(4)	20(6)	−8(3)	−8(3)	−7(5)		96
O(2)	96(g)		189(49)	189(49)	13580(52)	30(4)	30(4)	44(9)	−9(5)	−9(5)	19(6)		96
O(3)	96(g)		16923(33)	16923(33)	−3218(46)	26(4)	26(4)	27(6)	−3(4)	−3(4)	5(5)		96
O(4)	96(g)		18245(35)	18245(35)	32208(47)	31(4)	31(4)	32(7)	−8(4)	−8(4)	7(6)		96
La(I′)	32(e)	I′	6685(5)	6685(5)	6685(5)	35(1)	35(1)	35(1)	7(1)	7(1)	7(1)	32.7(7)	32
O(6)	32(e)		16444(43)	16444(43)	16444(43)	27(5)	27(5)	27(5)	−10(5)	−10(5)	−10(5)	35.4(21)	32
O(7)	16(c)		0	0	0	76(15)	76(15)	76(15)	−27(12)	−27(12)	−27(12)	21.1(22)	16
La(V)	16(d)	V	50000	50000	50000	213(18)	213(18)	213(18)	125(18)	125(18)	125(18)	6.0(4)	
O(5)	96(g)		20015(160)	20015(160)	43048(209)	93(18)						35.9(51)	
						(b) Crystal 2							
Si	192(i)		−5441(16)	3599(15)	12627(18)	17(2)	13(2)	16(2)	−4(2)	−4(2)	2(2)		192
O(1)	96(g)		−10644(43)	10644(43)	0	27(6)	27(6)	21(9)	−11(5)	−11(5)	2(8)		96
O(2)	96(g)		95(49)	95(49)	13571(63)	36(7)	36(7)	28(11)	−7(6)	−7(6)	30(9)		96
O(3)	96(g)		17044(39)	17044(39)	−3232(65)	14(5)	14(5)	50(11)	3(6)	3(6)	2(6)		96
O(4)	96(g)		18104(45)	18104(45)	32283(60)	32(6)	32(6)	31(9)	−17(6)	−17(6)	7(8)		96
La(I′)	32(e)	I′	6747(8)	6747(8)	6747(8)	33(1)	33(1)	33(1)	4(1)	4(1)	4(1)	28.0(4)	28
O(6)	32(e)		16478(66)	16478(66)	16478(66)	33(7)	33(7)	33(7)	−1(8)	−1(8)	−1(8)	47(3)	32
O(7)	16(c)		0	0	0	62(44)						12.6(21)	14
H3O(A)	32(e)	I′	4662(673)	4662(673)	4662(673)	30						7.8(27)	4
La(IV)	8(b)	IV	37500	37500	37500	93(13)						1.93(9)[e]	2[f]
O(9)	32(d)		31694(453)	31694(453)	31694(453)	120(65)						7.7(4)[e]	8[f]
La(V)	16(d)	V[g]	47949(75)	47949(75)	47949(75)	155(18)	155(18)	155(18)	96(18)	96(18)	96(18)	7.7(4)[e]	8[f]
O(5)	96(g)		51571(359)	51571(359)	39597(529)	123(44)						23.1(11)[e]	24[f]
O(8)	96(g)		55021(182)	55021(182)	42506(270)	30(17)						23.1(11)[e]	24[f]
H3O(B)	96(g)	III′	34865(585)	32956(576)	20444(493)	91(54)						23.1(11)[e]	24[f]
H3O(C)	32(e)	II	24000(202)	24000(202)	24000(202)	26(18)						10.6(16)	12[f]
						(c) Crystal 3							
Si	96(g)		−5587(14)	12610(15)	3540(13)	14(2)	14(2)	13(2)	−3(2)	−1(1)	−1(1)		96
Al	96(g)		−5595(13)	3578(14)	12507815)	8(2)	9(2)	10(2)	−3(2)	−1(1)	0(1)		96
O(1)	96(g)		−11087(35)	9(34)	10943(34)	25(5)	21(5)	17(5)	−9(4)	2(4)	−9(4)		96
O(2)	96(g)		−465(32)	−487(33)	13806(33)	14(5)	23(5)	18(5)	−3(4)	−10(4)	1(4)		96
O(3)	96(g)		−4077(36)	7849(35)	7604(36)	29(5)	16(5)	24(5)	5(4)	−9(4)	−0(4)		96
O(4)	96(g)		−6512(35)	6661(34)	18445(35)	23(5)	16(5)	25(5)	−5(4)	1(4)	−8(4)		96
La(I′)	32(e)	I′	6894(38)	6894(38)	6894(38)	116(5)	116(5)	116(5)	27(6)	27(6)	27(6)	7.5(3)	8[i]
OH2′	32(e)		17971(56)	17971(56)	17971(56)	38(6)	38(6)	38(6)	−1(7)	−1(7)	−1(7)	31.2(19)	24[i]
H_3O(A)	32(e)	II′	14430(158)	14430(158)	14430(158)	50[h]						5.3(11)	8[i]
La(II)	32(e)	II	23844(5)	23844(5)	23844(5)	13(0.5)	13(0.5)	13(0.5)	1.0(4)	1.0(4)	1.0(4)	23.6(3)	24[i]
H_3O(B)	32(e)	II	25612(235)	25612(235)	25612(235)	50[h]						8.9(19)	8[i]
W(1)	96(g)		31154(70)	22758(73)	31118(67)	72(13)	70(13)	57(11)	−8(10)	−39(10)	−16(10)	77(4)	72[i]
W(2)	96(g)		38322(680)	17087(392)	36790(619)	59(13)[j]						10.2(19)	16[k]
W(3)	96(g)		42361(251)	19669(223)	26844(237)	59(13)[j]						23(3)	24[k]
W(4)	96(g)		44868(194)	16266(194)	22380(193)	59(13)[j]						25(3)	24[k]
W(5)	96(g)		38958(417)	20651(391)	28840(377)	59(13)[j]						13(3)	16[k]
La(V)	32(e)	V[g]	46145(377)	46145(377)	46145(377)	20[h]						1.1(3)	

[a] Positional parameters are given $\times 10^5$. [b] Thermal parameters are given $\times 10^3$. Numbers in parentheses are the esd's in the units of the least significant digit given for the corresponding parameter. [c] The anisotropic temperature factor = $\exp[-2\pi^2 a^{-2}(h^2U_{11} + k^2U_{22} + l^2U_{33} + 2klU_{23} + 2hlU_{13} + 2hkU_{12})]$. [d] Occupancy factors are given as the number of atoms or ions per unit cell. [e] These values were constrained in final least-squares refinement to the ratio 1:4:4:12:12:12, respectively. [f] These values were not used in least-squares refinement. These occupancies allow for charge balance. [g] The La(V) position is actually 0.89(3) Å (crystal 2) and 1.63(15) Å (crystal 3) from site V (0.5, 0.5, 0.5) along the 3-fold axis. [h] These values were fixed in final least-squares refinement due to unusual U_{iso} values. [i] These values were fixed in final least-squares refinement to the ratio 1:3:1:3:1:9, respectively. [j] Constrained to be equal. [k] These occupancies were not used in least-squares refinement.

Isotropic refinement including La(V), a large peak at (0.48, 0.48, 0.48) found on a subsequent Fourier function, converged with $R_1 = 0.15$ and $wR_2 = 0.37$. Anisotropic refinement of the framework atoms, La(I′), and O(6), converged with $R_1 = 0.14$ and $wR_2 = 0.34$. Similarly, from a subsequent difference Fourier function, a peak at (0.0, 0.0, 0.0) was introduced as O(7). This refinement converged with $R_1 = 0.13$ and $wR_2 = 0.35$.

The difference Fourier function revealed peaks at (0.40, 0.52, 0.52) and (0.43, 0.55, 0.55), and their isotropic refinement as O(5) and O(8) converged with $R_1 = 0.12$ and $wR_2 = 0.32$. Because the occupancy at O(6) was refining to greater than full occupancy, it was constrained to be full. The error indices remained unchanged.

Anisotropic thermal parameter refinement for La(V) converged to $R_1 = 0.11$ and $wR_2 = 0.30$. Because the occupancies at La(V), O(5), and O(8) were refining nearly in the ratio of 1:3:3, this constraint was added: $R_1 = 0.11$ and $wR_2 = 0.31$. A new difference Fourier function revealed peaks at (0.375, 0.375, 0.375) and (0.32, 0.32, 0.32), and their isotropic refinement as La(IV) and O(9) converged with $R_1 = 0.094$ and $wR_2 = 0.27$. Similarly, from a subsequent difference function, two peaks at (0.35, 0.33, 0.20) and (0.24, 0.24, 0.24) were introduced as H_3O-(B) and H_3O(C); refinement converged with $R_1 = 0.092$ and $wR_2 = 0.25$. Constraining the occupancies at La(IV), O(9), La-(V), O(5), O(8), and H_3O(B) to the ratio 1:4:4:12:12:12, respectively, had no effect on the *R* values (see Table 2b).

TABLE 3: Selected Interatomic Distances (Å) and Angles (deg)[a] for Crystals 1 and 2

	crystal 1	crystal 2
(Si,Al)−O(1)	1.651(5)	1.661(7)
(Si,Al)−O(2)	1.665(5)	1.659(6)
(Si,Al)−O(3)	1.699(5)	1.694(7)
(Si,Al)−O(4)	1.653(5)	1.667(7)
O(1)−(Si,Al)−O(2)	114.4(5)	114.3(7)
O(1)−(Si,Al)−O(3)	113.0(5)	113.6(6)
O(1)−(Si,Al)−O(4)	109.2(6)	107.3(7)
O(2)−(Si,Al)−O(3)	98.6(6)	99.6(8)
O(2)−(Si,Al)−O(4)	111.0(6)	112.1(8)
O(3)−(Si,Al)−O(4)	110.3(6)	109.9(7)
(Si,Al)−O(1)−(Si,Al)	143.5(8)	139.8(10)
(Si,Al)−O(2)−(Si,Al)	148.7(9)	149.9(12)
(Si,Al)−O(3)−(Si,Al)	141.6(8)	141.6(11)
(Si,Al)−O(4)−(Si,Al)	136.5(8)	137.7(9)
La(I′)−O(2)	2.872(13)	2.913(17)
La(I′)−O(3)	2.524(12)	2.538(17)
La(I′)−O(6)	2.528(7)	2.517(10)
La(I′)−O(7)	2.895(2)	2.929(3)
O(4)−O(5)	2.78(5)	2.63(12)
La(V)−O(5)	2.48(6)	2.46(12)
La(V)−O(8)		2.61(7)
O(3)−O(7)	2.967(12)	2.933(14)
O(4)−O(8)		2.65(7)
H_3O(A)−O(2)		2.69(3)
H_3O(A)−O(3)		2.41(5)
H_3O(B)−O(5)		2.77(18)
H_3O(B)−O(8)		2.74(16)
H_3O(C)−O(2)		2.63(4)
La(IV)−O(9)		2.52(20)
O(9)−H_3O(B)		2.95(13)
O(9)−H_3O(C)		3.34(21)
O(3)−La(I′)−O(3)	104.6(6)	102.7(4)
O(3)−La(I′)−O(6)	91.3(3), 91.3(3), 153.6(5)	91.1(5), 92.1(5), 155.8(7)
La(I′)−O(6)−La(I′)	108.8(4)	108.1(6)
O(3)−La(I′)−O(7)	66.0(4)	64.4(3)
O(6)−La(I′)−O(7)	140.4(4)	139.7(6)
O(5)−La(V)−O(5)	63.0(7),117.0(7)	119.6(7)
O(8)−La(V)−O(8)		116.1(10)
O(5)−La(V)−O(8)		61.7(9),172(3)
O(2)−H_3O(C)−O(2)		99(2)
O(8)−H_3O(B)−O(9)		119(5)
O(9)−La(IV)−O(9)		109.50(1)

[a] The numbers in parentheses are the esd's in the units of the least significant digit given for the corresponding parameter.

Fixing the occupancy at La(I′) at 32 per unit cell caused the R's to increase and the occupancy of the La(IV)-centered cluster to become less rational; it increased from 1.9 to 2.3. One more peak at (0.046, 0.046, 0.046) from a difference Fourier function refined isotropically as H_3O(A) with $R_1 = 0.091$ and $wR_2 = 0.25$. However, the occupancy at O(7) became small, only 8.7-(16). When the occupancy at La(I′) was fixed at 28 per unit cell, the occupancy at O(7) became 12.7(7). The occupancy at O(7) was fixed at 14 because the 28 La^{3+} ions at La(I′) can bind to 14 water molecules at O(7). This did not affect the *R* values: $R_1 = 0.091$ and $wR_2 = 0.250$.

The goodness-of-fit is 1.125 (see Table 1). The largest residual peak on the final difference Fourier function appeared at (0.27, 0.27, 0.27). This peak was discarded because it was too close to H_3O(C) (1.3 Å) and to O(9) (1.74 Å) to be in a supercage that contains a major cluster and too far from the zeolite framework (about 3.4 Å) to be alone in an otherwise empty supercage. The final refinement was done with the recommended value of *a* in the weighting scheme: $R_1 = 0.091$ and $wR_2 = 0.253$. The final structural parameters and selected interatomic distances and angles are presented in Tables 2b and 3, respectively.

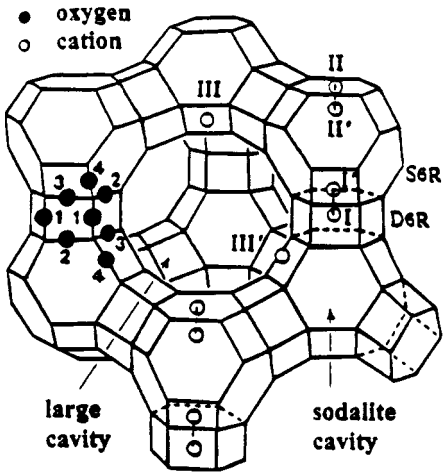

Figure 1. Stylized drawing of the framework structure of zeolite X. Near the center of each line segment is an oxygen atom. The different oxygen atoms are indicated by the numbers 1−4. Si and Al atoms alternate at the tetrahederal intersections, except that Si substitutes for Al at about 4% of the Al positions. Extraframework cation positions are labeled with Roman numerals. Not shown are sites IV (at the center of the large cavity or supercage) and V (at the 12-ring centers).

3. Crystal 3 (Fully Hydrated). Full-matrix least-squares refinement[24] began with the framework coordinates of dehydrated Na−X.[27] Isotropic refinement of the framework atoms yielded $R_1 = 0.60$ and $wR_2 = 0.89$. A difference Fourier function revealed a large peak at (0.238, 0.238, 0.238). Isotropic refinement including this peak as La(II) converged with $R_1 = 0.15$ and $wR_2 = 0.41$.

Isotropic refinement including two peaks at (0.069, 0.069, 0.069) and (0.179, 0.179, 0.179) found on a subsequent difference function, converged with $R_1 = 0.12$ and $wR_2 = 0.32$. Anisotropic refinement of framework atoms and these two positions as La(I′) and OH2′ converged with $R_1 = 0.12$ and $wR_2 = 0.32$. Similarly, from a new difference Fourier function, two peaks at (0.228, 0.311, 0.311) and (0.171, 0.382, 0.367) were introduced as W(1) and W(2). These added isotropically to refinement converged with $R_1 = 0.092$ and $wR_2 = 0.26$. Anisotropic thermal parameter refinement for La(I′), OH2′, and La(II) converged with $R_1 = 0.091$ and $wR_2 = 0.25$. H_3O(A) was found on a subsequent Fourier function; when added to the model and refined isotropically, $R_1 = 0.088$ and $wR_2 = 0.24$ resulted.

The next difference Fourier function revealed peaks at (0.163, 0.225, 0.449) and (0.206, 0.288, 0.392), and their isotropic refinement as W(4) and W(5) converged with $R_1 = 0.081$ and $wR_2 = 0.23$. A new difference Fourier function revealed peaks at (0.256, 0.256, 0.256) and (0.197, 0.266, 0.425). Their isotropic refinement as H_3O(B) and W(3) and anisotropic refinement of W(1) converged with $R_1 = 0.0760$ and $wR_2 = 0.220$. Fixing the thermal parameters of H_3O(A) and H_3O(B) at 0.05 Å^2 because of unusual U_{iso} values, 0.38 Å^2 and a negative value, respectively, had no effect on the *R* values. Fixing the occupancies at La(I′), OH2′, H_3O(A), H_3O(B), La(II), and W(1) to the ratio 1:3:1:1:3:9, respectively, caused the error indices to increase a little: $R_1 = 0.0781$ and $wR_2 = 0.222$ (see Table 3c). The largest residual peak on the next difference Fourier function appeared at (0.4815, 0.4815, 0.4815); with its thermal parameter fixed at 0.20 Å^2, refinement as La(V) converged with $R_1 = 0.0775$ and $wR_2 = 0.2205$. Because the U_{iso} value for W(2) was small, 0.008(27) Å^2, U_{iso} for W(2), W(3), W(4), and W(5) were constrained to be equal in the final refinements.

The goodness-of-fit is 1.084 (see Table 1). The next largest peak at (0.4189, 0.4189, 0.4189) was discarded because the

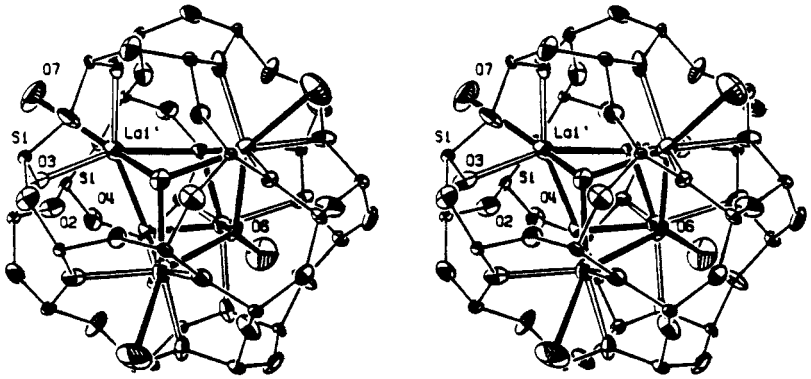

Figure 2. Stereoview of a sodalite cage with attached O(7) in double six-rings (D6R's) in crystal 1. Four La^{3+} ions at La(I′) are bound to four O^{2-} ions at O(6) and four at O(7). Thin bonds indicate the framework; heavy bonds indicate a portion of the La_2O_3 continuum in and about a sodalite cage. Ellipsoids of 50% probability are shown.

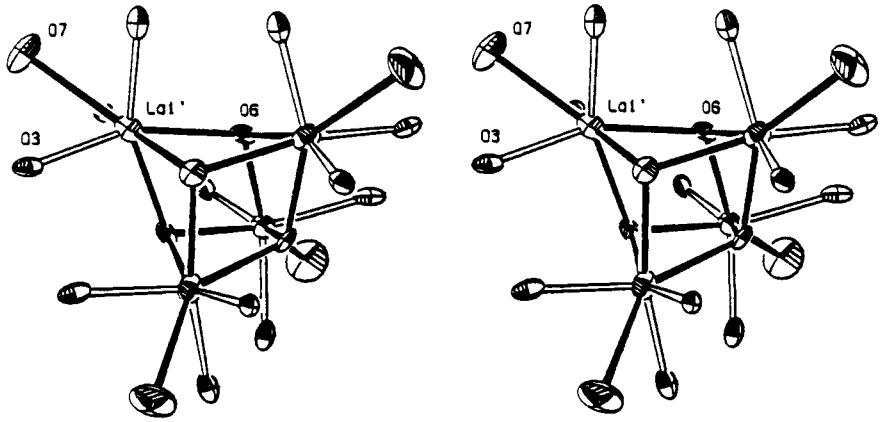

Figure 3. Stereoview of the contents of a sodalite cage and of its four adjacent double six-rings (D6R's) in crystal 1. For clarity, the framework is omitted. Four La^{3+} ions at La(I′) are bound to four O^{2-} ions at O(6) and four at O(7). Open bonds are drawn to the framework oxygens, and heavy bonds indicate the cubic continuum. Ellipsoids of 50% probability are shown.

occupancies became negligible in refinement. The final refinement was done with the recommended value of a in the weighting scheme; $R_1 = 0.0774$ and $wR_2 = 0.2199$. The final structural parameters and selected interatomic distances and angles are presented in Tables 2c and 4, respectively.

Description of the Structures

1. Description of Zeolite X. Zeolite X is a synthetic counterpart of the naturally occurring mineral faujasite (see Figure 1). The cuboctahedron (14-hedron with 24 vertexes) known as the sodalite cavity or β-cage may be viewed as its principle building block. These β-cages are connected tetrahedrally at six-rings by bridging oxygens to give double six-rings (D6R's, hexagonal prisms) and concomitantly to give an interconnected set of even larger cavities (supercages) accessible in three dimensions through 12-ring (24-membered) windows. The Si and Al atoms occupy the vertexes of these polyhedra. The oxygen atoms lie approximately midway between each pair of Si and Al atoms, but are displaced from those points to give near tetrahedral angles about Si and Al. Single six-rings (S6R's) are shared by sodalite and supercages and may be viewed as the entrances to the sodalite units. Each unit cell has eight sodalite units, eight supercages, 16 D6R's, 16 12-rings, and 32 S6R's.

Exchangeable cations that balance the negative charge of the aluminosilicate framework are found within the zeolite's cavities. They are usually found at the following sites shown in Figure 1: site I at the center of a D6R, I′ in the sodalite (β) cavity on the opposite side of one of the D6R's six-rings from site I, II′ inside the sodalite cavity near a S6R, II in the supercage adjacent to a S6R or at the center of the S6R, III in the supercage opposite a four-ring between two 12-rings, and III′ somewhat or substantially distant from III but otherwise near the inner walls of the supercage or the edges of 12-rings. Site IV at the very center of the supercage, and site V at a 12-ring center between two supercages are unusual cation sites not often occupied because the cationic charge would be far from the anionic zeolite framework.[28,29]

2. Crystal 1 (Vacuum Dehydrated at 400 °C). La^{3+} ions occupy only two crystallographic sites. Thirty-two fill site I′ (in the sodalite units). The remaining six La^{3+} ions are found at site V (at the centers of 12-rings).

A tetrahedron of four La^{3+} ions at site I′ is found in each sodalite unit; each La^{3+} ion coordinates to three O(3) framework oxygens. This tetrahedron is interpenetrated by a tetrahedron of four nonframework oxide ions at O(6) to give a distorted La_4O_4 cube (see Figures 2 and 3). The La^{3+} tetrahedron is larger than the O^{2-} tetrahedron to minimize repulsions. The cubes are linked at each corner by additional nonframework oxide ions at O(7) to form a neutral La_2O_3 continuum (see Figure 4). The coordination at each La^{3+} ion at I′ is trigonally distorted monocapped octahedral[30−34] with three La(I′)−O(3) distances of 2.524(12) Å, three La(I′)−O(6) distances of 2.528(7) Å, and a much longer (capping) La(I′)−O(7) distance, 2.895(2) Å. The same coordination geometry is seen in the crystal structure of La_2O_3, but the bond distances there are very different: three at 2.38 Å, three at 2.72 Å, and one at 2.45 Å (electron diffraction results; no esd's given).[34,35] The average La−O bond distance

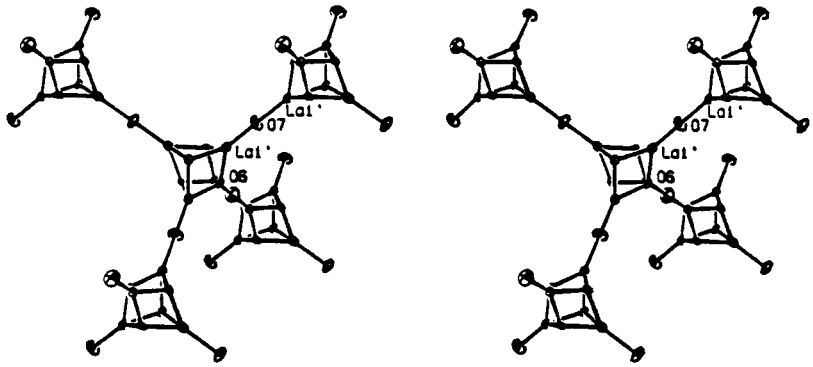

Figure 4. Stereoview of a portion of the La_2O_3 continuum in crystal 1. For clarity, the framework is omitted. Other details are the same as for Figure 3.

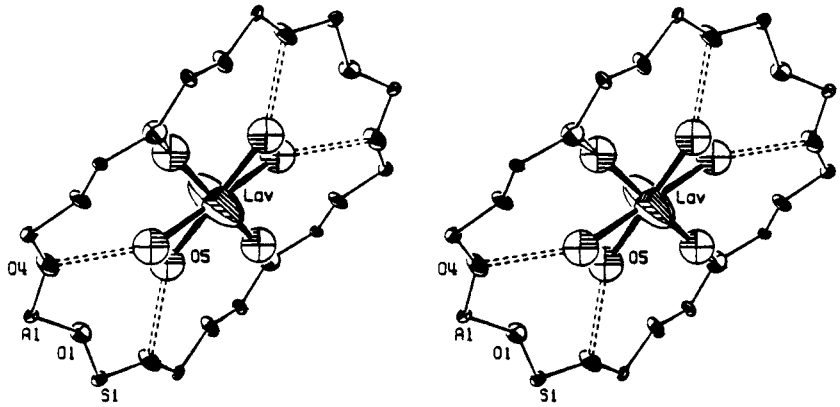

Figure 5. Stereoview of a 12-ring containing a hexacoordinate La^{3+} ion at site V in crystal 1. Thin bonds indicate the zeolite framework and heavy bonds indicate coordination about La(V). Ellipsoids of 50% probability are shown.

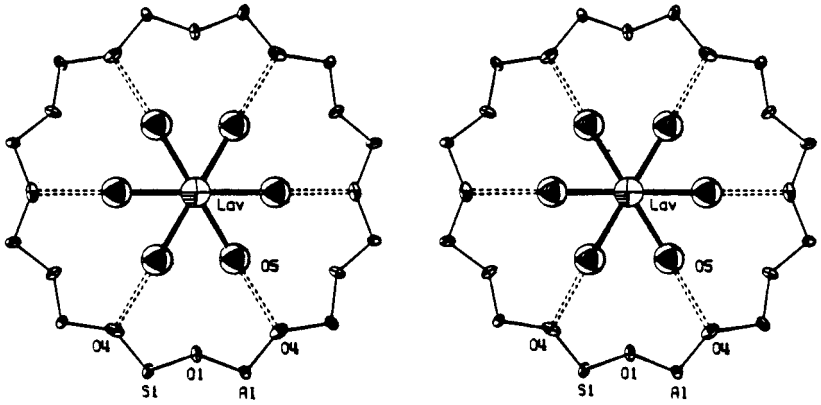

Figure 6. Stereoview along the 3-fold axis of a 12-ring containing a hexacoordinate La^{3+} ion at site V in crystal 1. Other details are the same as for Figure 5.

in La_2O_3, 2.54 Å, is a little less than that found for the intrazeolitic La_2O_3 continuum, 2.58 Å. The precisely determined crystal structure[36] of Ce_2O_3 (isostructural with La_2O_3) supports the La_2O_3 structure[35] referenced above; the mean Ce−O distance (2.505 Å) corrected for the lanthanide contraction (1.061−1.034 = 0.027 Å) is 2.532 Å, approximately 2.54 Å.[35] For Pr_2O_3 (also isostructural),[37] this value is 2.483 + 0.048 = 2.531 Å. For comparison, the sum of the ionic radii of La^{3+} and O^{2-}, 1.061 + 1.32, is 2.381 Å.[38]

The remaining six La^{3+} ions at site V (0.5, 0.5, 0.5) are bound to six oxygens, presumeably three OH^- and three H_2O molecules, all six of which hydrogen bond at 2.78(5) Å to framework oxygens at O(4) (see Figures 5 and 6). Because La-(V) does not approach framework oxygens, it is presumed that it has its charge balanced by three OH^- ions; to avoid the very low coordination number three, it appears to have retained three water molecules, even after vacuum dehydration at 400 °C.

3. Crystal 2 (Vacuum Dehydrated at 22 °C). La^{3+} ions are found at three crystallographic sites: I′, IV, and V. Twenty-eight La^{3+} ions seven-eights fill the 32-fold site I′ (in the sodalite units), eight of the remaining 10 are found near site V, and the final two are at site IV. A hydronium ion occupies a different site I′ in four of the eight sodalite cages. Because the occupancy at La(I′) is 28, and consistent with the occupancy of 14 at O(7), half of the sodalite units contain complete $La_4(OH)_4^{8+}$ "cubes," and the other half contain $La_3(OH)(OH_2)_3^{8+}$ units, cubes with one corner (a La^{3+} ion) missing (see Figures 7−9). The nonfilling of site I′ is apparently a result of the high concentration of H^+ and the presence of water; this discourages the completion of the La_2O_3 continuum found in crystal 1.

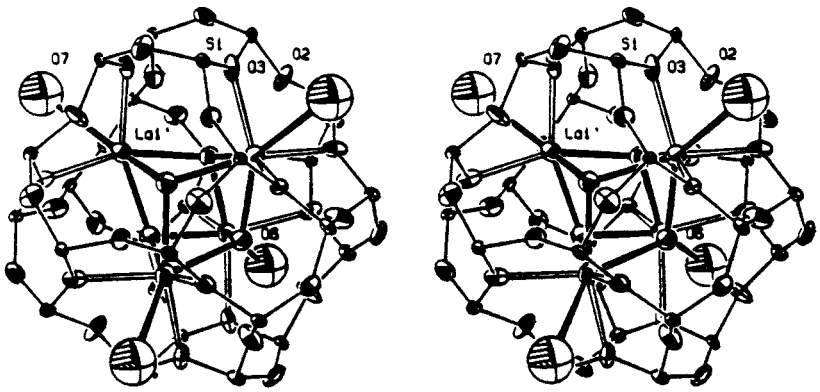

Figure 7. Stereoview of a sodalite cage with attached O(7) in double six-rings (D6R's) in crystal 2. Four La^{3+} ions at La(I′) are bound to four OH^- ions at O(6) and four water molecules at O(7). Thin bonds indicate the framework and heavy bonds indicate the continuum within the sodalite cage. Ellipsoids of 50% probability are shown.

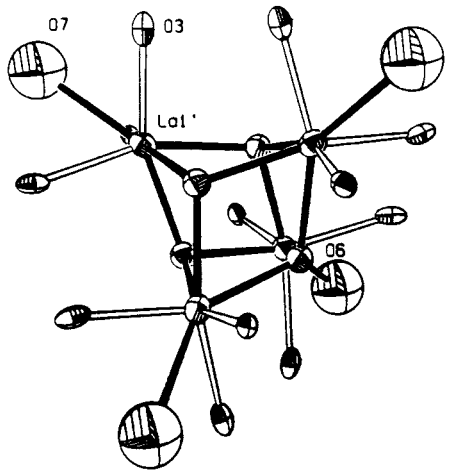

Figure 8. The contents of a sodalite cage and of its four adjacent double six-rings (D6R's) in crystal 2. Except for the O(3) atoms, the framework is omitted for clarity. Four La^{3+} ions at La(I′) bind multiply to four OH^- ions at O(6) and singly to four water molecules at O(7) which bridge to other such clusters. Open bonds are to O(3) oxygens of the zeolite framework, and heavy bonds indicate the La_2O_3 continuum. Ellipsoids of 50% probability are shown.

All of the La^{3+} ions at site IV and near site V cluster, with OH^-, H_2O, and H_3O^+, to fill two of the eight supercages per unit cell (see Figures 10−12). Each consists of a La^{3+} ion at site IV, four La^{3+} ions at site V, 19 coordinating water molecules, and six H_3O^+ ions at site III′. Each La^{3+} ion at site IV (supercage center) is coordinated tetrahedrally by four O(9) oxygens. Because these La^{3+} ions are very distant from the anionic zeolite framework, three of these should be OH^- ions. Similarly, each La^{3+} ion near site V (0.89(3) Å from site V) is coordinated in a near hexagonal-planar manner by three water molecules and three hydroxide ions, all six of which hydrogen bond (three at 2.63(12) Å and three at 2.65(7) Å, respectively) to O(4) framework oxygens (see Figures 13 and 14). Because H_2O coordinated to La^{3+} should be much more acidic than coordinated OH^-, therefore able to hydrogen bond more strongly to O(4) and have a smaller thermal parameter, O(8) appears to be H_2O and O(5) appears to be OH^- (see Figure 14). (The single thermal parameter for the corresponding oxygens in crystal 1 is nicely intermediate in magnitude (see Figure 6)). Six H_3O^+ ions and six water molecules surround each site-IV $La(OH)_3OH_2$ molecule and bridge to 12 O(5) oxygens and to another 12 O(8) oxygens near La(V) to form the large supercage clusters. Also, 12 H_3O^+ ions are distributed among the other six supercages.

4. Crystal 3 (Fully Hydrated). In this structure, La^{3+} ions are found at three crystallographic sites: I′, II, and V. Eight lie at site I′ (in the sodalite units), 24 are found at site II, and the remaining one lies at site V. Filling site II′ (in the sodalite cages) are 24 OH^- ions at OH2′ and eight H_3O^+ ions at H_3O(A). Because the occupancies at La(I′) and OH2′ are 8 and 24, respectively, each sodalite unit contains a $La(OH)_3$ molecule at site I′; La(I′) coordinates octahedrally to three OH^- and three O(3) framework oxygens (see Figure 15). Each OH^- ion bridges to a La^{3+} ion at site II. Because the occupancy at H_3O(A) is eight per unit cell, each triplet of OH^- ions is capped by a H_3O^+ ion with three hydrogen bonds at 2.78(5) Å.

Each supercage contains three La^{3+} ions at site II and 19 water molecules. Each La^{3+} ion coordinates to a bridging hydroxide ion at OH2′, to three O(2) framework oxygens, and to three water molecules at W(1) in a trigonally capped trigonal-prismatic manner (see Figure 16). One or two water molecules per supercage at W(2) bridge between W(1) molecules. Another eight water molecules, three at W(3), three at W(4), and two at W(5) hydrogen bond to O(1) framework oxygens at 2.74(6), 2.68(5), and 2.70(10) Å, respectively. W(3) and W(4) can also hydrogen bond to W(2) at 2.78(15) and 2.51(16) Å, respectively. One hydronium ion per supercage, H_3O(B) at site II, hydrogen bonds to three O(4) framework oxygens.

Discussion

Complete La^{3+}-exchange of single crystals of Na_{92}−X was attempted using near neutral aqueous solution at 90 °C. All Na^+ ions were successfully removed; consistent with the results of microprobe analysis, no Na^+ ions were found crystallographically in any of the three crystals. All crystals were overexchanged; in each case, the sum of the La^{3+} charges is more than the 92+ needed to balance the framework charge. Crystals 1 and 2 have the same number of La^{3+} ions, 38 per unit cell, but only 33 are found in the fully hydrated crystal (crystal 3). Because the ion-exchange pH for crystal 3 was ca. 0.56 units less than that for crystals 1 and 2, crystal 3 should have fewer OH^- groups and the extent of overexchange should be diminished. By extrapolation, a pH of 6.78 might yield La_{32}−X, an ideal composition for preparing a complete La_2O_3 continuum with no excess La^{3+} species.

Crystal 1 was evacuated at 400 °C. With a framework charge of 92 and 38 La^{3+} ions per unit cell, $38(+3) - 92 = 22$ additional negative charges, as oxide or hydroxide, are needed for charge balance. However many more such anions are found per unit cell. If the 84 extraframework oxygens are taken to be 32 oxide ions μ_3-coordinated to La(I′), 16 oxide ions μ_2-coordinated to La(I′), 18 hydroxide ions coordinated to La(V),

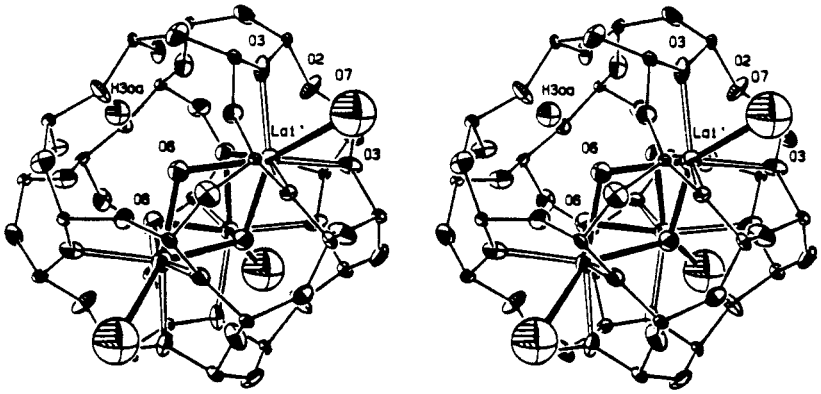

Figure 9. Stereoview of the remaining sodalite cages in crystal 2 with attached O(7)'s in double six-rings (D6R's). Three La^{3+} ions at La(I′) are bound to four OH^- ions at O(6) and also to three O(7)'s. The H_3O^+ ions at site I′ are off the site I′ of the La^{3+} ions. Ellipsoids of 50% probability are shown.

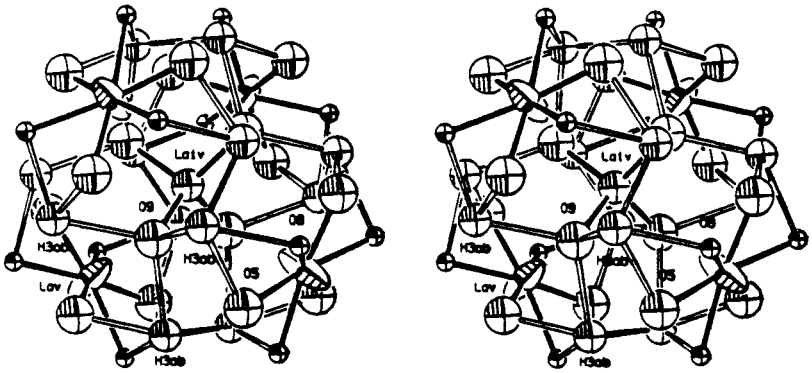

Figure 10. Stereoview of the large supercage cluster in crystal 2. About two of the eight supercages per unit cell contain this cluster; the remainder are relatively empty. A La^{3+} ion at site IV (the center of the supercage) is coordinated tetrahedrally by four O(9) oxygens. Each La(V) ion is actually 0.89(3) Å from site V and is coordinated in a near hexagonal-planar manner by three H_2O molecules and three OH^- ions at O(5) and O(8). Which three are at O(5) and which three are at O(8) has not been determined. Ellipsoids of 50% probability are shown.

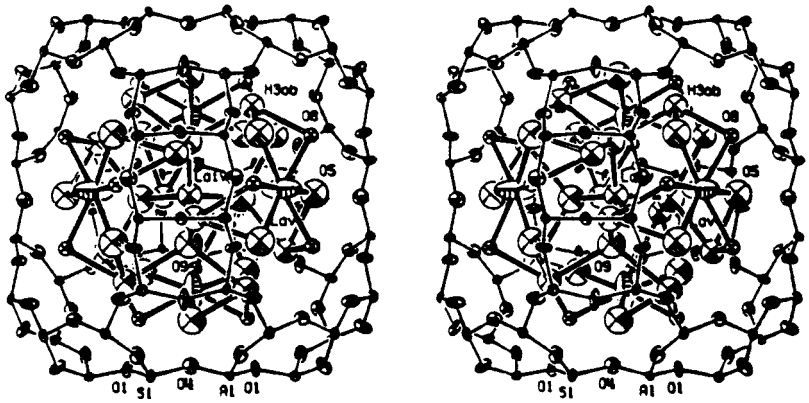

Figure 11. Stereoview showing the positioning of the cluster shown in Figure 10 in its supercage. Other details are the same as for Figure 10.

and 18 water molecules also coordinating to La(V), then it may be said that the number of anions retained by the zeolite is sufficient, 114, to balance the charges of all 38 La^{3+} ions per unit cell. Most conspicuous would be the 48 oxide ions which, with 32 of the 38 La^{3+} ions per unit cell, would form a neutral La_2O_3 continuum (Figure 4) which extends through all sodalite units and D6R's. The only water molecules that remain (It is surprising that there are any after vacuum dehydration at 400 °C.) coordinate to site-V $La(OH)_3$ molecules, maintaining their coordination numbers at six (Figures 5 and 6). The entire anionic charge of the zeolite framework would be balanced by protons (unlocatable in this work). These protons should associate with oxygens of the anionic zeolite framework and seem more sensibly placed in the supercages into which the framework oxygens extend. There is adequate space in the supercages; the sodalite units and D6R's are quite full with the La_2O_3 continuum. This system may have structurally factored itself into three neutral substructures: the La_2O_3 continuum, the zeolite framework in its hydrogen form, and hydrated $La(OH)_3$ molecules. Per unit cell, this is $La_{32}O_{48}$, $H_{92}Si_{100}Al_{92}O_{384}$, and six near planar molecules of $La(OH)_3(OH_2)_3$. It remains possible that some of the protons associate with oxide ions of the continuum.

Crystal 2 was evacuated at 22 °C. Extensive hydrolysis of La^{3+} is seen to give 50 OH^- and 28 H_3O^+ ions per unit cell. With 38 La^{3+} ions and the anionic charge of the zeolite framework, charge balance is achieved. Among the H_3O^+ ions, four per unit cell at site I′ prevent the completion of a La_2O_3 continuum. Sixty-four undissociated water molecules remain per unit cell.

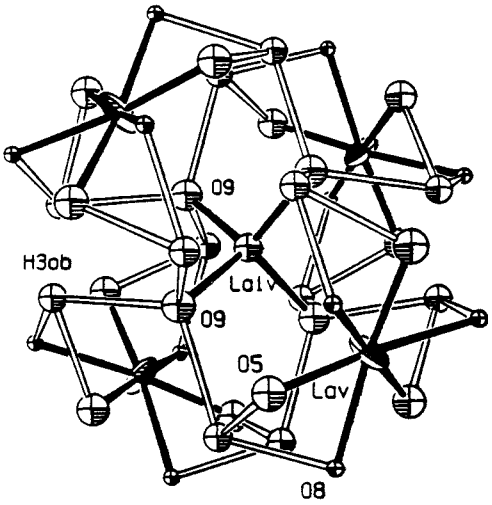

Figure 12. Another view of the supercage cluster in crystal 2. For clarity, it is shown here without its supercage using ellipsoids of lesser (20%) probability. A La^{3+} ion at site IV (the center of the supercage) is coordinated tetrahedrally by four O(9) oxygens. Other details are the same as for Figure 10.

Crystal 3 was not evacuated at all; it was studied in its fully hydrated form. A lesser degree of La^{3+} hydrolysis is seen as compared to crystal 2: 24 OH^- and 16 H_3O^+ ions are found per unit cell. With 33 La^{3+} ions and the anionic charge of the zeolite framework, charge balance is almost achieved; hydroxide ions that must coordinate to La(V) have not been found or considered. In the supercages, about 152 water molecules per unit cell are found at five equipoints (see Table 3c).

The distributions of La^{3+} ions in the dehydrated crystals (1 and 2) are similar; most La^{3+} ions are at site I′ (in the sodalite units). In crystal 1, 32 La^{3+} ions preferentially occupy and fill site I′; the remaining six La^{3+} ions are at site V. In crystal 2, 28 occupy site I′, eight are found at site V, and the remaining two are at site IV. In the hydrated structure, however, only eight La^{3+} ions are found at site I′; most La^{3+} ions are in the supercages. Site II is the most populated with 24 La^{3+} ions, and only one La^{3+} ion is found at site V.

The H_3O^+ ions are distributed quite differently in crystals 2 and 3. It appears that they are distributing themselves to best balance the charges within the zeolite after the La^{3+} ions have selected their ligands and positions. In crystal 2, 12 H_3O^+ ions preferentially occupy site III′, 12 are at site II, and only four are at site I′; in crystal 3, sites II′ and II each contain eight H_3O^+ ions.

Apparently the hydrolysis of La^{3+} ions in solution generates H_3O^+ ions, some of which exchange into the zeolite. In addition, vacuum dehydration at 22 °C promotes the hydrolysis of hydrated La^{3+} ions in the zeolite. No H_3O^+ ions were found in the 400 °C vacuum-dehydrated crystal. Apparently all H_3O^+ ions had decomposed,

$$H_3O^+ \rightarrow H^+ + H_2O$$

and the reaction

$$2La^{3+} + 3H_2O \rightarrow La_2O_3 + 6H^+$$

had gone to completion to form the La_2O_3 continuum. Only those water molecules that were needed to complete the coordination spheres of the site-V (12-ring) La^{3+} ions were retained.

The neutral La_2O_3 continuum is remarkable (see Figures 3 and 4). (A continuum is defined as a large number of atoms bonded together, excluding hydrogen bonds, throughout a phase.) It is the first binary and the first neutral intrazeolitic continuum to be reported. (Cationic cesium,[28,29] rubidium, [39] and potassium[40] continua have been found.) Two-thirds of its oxygens, O(6), μ_3-bridge between three La^{3+} ions (see Figure 4), and the remainder, O(7), are exactly (linearly) between two La^{3+} ions. Neither kind of oxygen should associate with hydrogen ions (not located in this work): each of the first kind is already heavily coordinated (by three La^{3+} ions) and the second would have been shifted from site I to a position of lower symmetry. This La_2O_3 continuum has formed within the anionic zeolite continuum, allowing the zeolite to be more hydrothermally robust while simultaneously releasing many H^+ ions active in acid catalysis. Because the oxides of the first four lanthanides (La_2O_3,[35] Ce_2O_3,[36] Pr_2O_3,[37] and Nd_2O_3[41]) are isostructural,[34] the latter three might be expected to form similar continua within zeolite X unless the lanthanide contraction leads to an unacceptable fit. Other large 3+ cations (other lanthanides, actinides, etc.) may do so also. If a lanthanide continuum could be doped, perhaps by using a mixed ion-exchange solution initially, zeolitic materials with novel frequency-doubling, ion-conducting, and catalytic properties such as those seen with La_2O_3[6−10] might be prepared.

In all three crystals, La^{3+} ions are found on 3-fold axes at or near site V (12-ring centers) (Figures 5, 6, 13, and 14). Because these La^{3+} ions are far from the anionic zeolite framework, their charge must be immediately balanced by other anions. Because only oxygen anions are available, because this is seen at all states of hydration, and because La(V) lies on a 3-fold axis, these must be trigonally arranged hydroxide ions. Near hexagonal planar coordination is found on 3-fold axes in crystals 1 and 2: $La(OH)_3(OH_2)_3$ appears to be more reasonable than $La(OH)_6^{3-}$ which should show much stronger departures from trigonal planar toward octahedral. Even after vacuum dehydration at 400 °C, $La(OH)_3(OH_2)_3$ has retained its three H_2O molecules, apparently to avoid a reduction in coordination number. In crystal 2, $La(OH)_3(OH_2)_3$ is pulled off site V by a small amount, 0.89 Å, because of a further interaction on one side. (For crystal 3, the occupancy at La(V) is very low and its coordination sphere is not found; La(V) is 1.63(15) Å from its 12-ring plane.) This near-hexagonal-planar coordination suggests that the six ligands are delocalizing electron density into La^{3+}'s empty $4f_{x(x^2-3y^2)}$ orbital which has six coplanar lobes. The Ce−OH infrared bands found by Rabo et al. in Ce−Y that had been vacuum dehydrated at 500 °C[19] could be due to hydrated $Ce(OH)_3$ in 12-rings, like the $La(OH)_3(OH_2)_3$ molecules found here. This six-coordinate planar coordination geometry had not been previously reported for any cation.

Benzene molecules are similar to $La(OH)_3(OH_2)_3$ in size and symmetry. Of course they are also neutral. They occupy the same 12-ring positions in zeolites X and Y[42−44] as $La(OH)_3(OH_2)_3$ molecules do here (see Figures 5 and 6).

In crystal 2, hydrolyzed La^{3+} ions are found even further, as far away as they can be, from the zeolite framework, at the centers of two of the eight supercages per unit cell (see Figures 10−12). Each is coordinated tetrahedrally by four oxygens. As with the 12-ring site-V La^{3+} ions, because these La^{3+} ions are so distant from the anionic zeolite framework, three of these oxygens should be OH^- ions ($La(OH)_3OH_2$); $La(OH)_4^-$ is also possible. Each site-IV La^{3+} ion has a secondary coordination sphere of six H_2O molecules and six H_3O^+ ions. It is remarkable to see such highly charged cations (La^{3+}) so far from the anionic

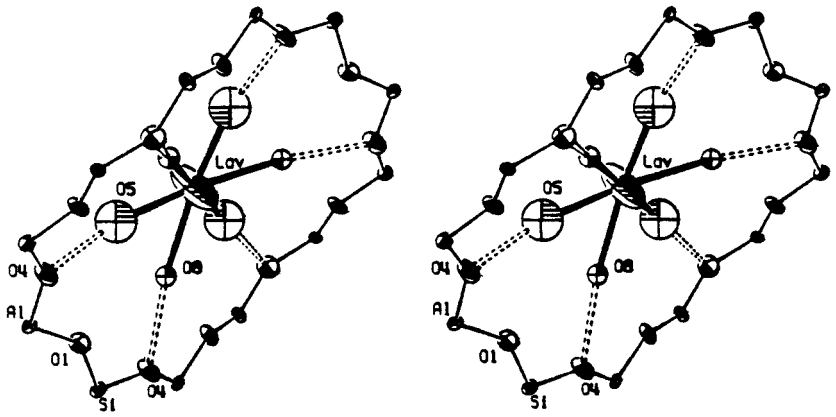

Figure 13. Stereoview of a 12-ring containing a hexacoordinate La^{3+} ion at site V in crystal 2. Other details are the same as for Figure 5.

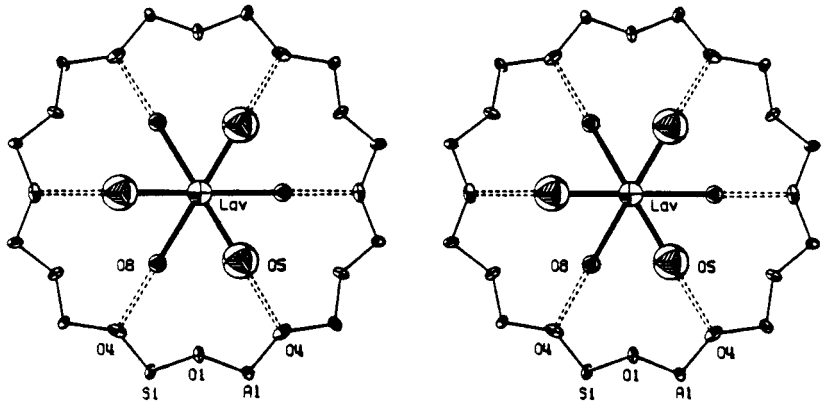

Figure 14. Stereoview along the 3-fold axis of a 12-ring containing a hexacoordinate La^{3+} ion at site V in crystal 2. Other details are the same as for Figure 5.

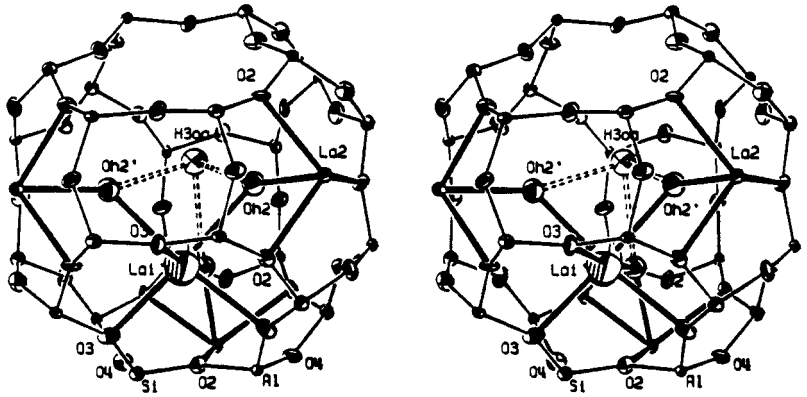

Figure 15. Stereoview of the sodalite unit in crystal 3. A La^{3+} ion at La(I′) bonds to three OH^- ions at OH2′. Each of these hydroxide ions bridges to a La(II) ion. The La(II) ions each coordinate further to three water molecules at W(1) (not shown), outside the sodalite cavity. The H_3O^+ ion at another II′ site, H_3O(A), hydrogen bonds triply to the three hydroxide ions at OH2′. Ellipsoids of 50% probability are shown.

zeolite framework and to see each of these La^{3+} ions use the entire volume of a supercage to construct both its own primary coordination sphere and a secondary coordination sphere which hydrogen bonds through a third coordination sphere to the zeolite framework (see Figure 11).

Neither of these La^{3+} coordination geometries, neither six-coordinate planar (or near planar) nor tetrahedral, is seen in the structure of $La(OH)_3$, nor those of other lanthanide hydroxides.[47] All lanthanide metal hydroxides display nine-coordinate tricapped trigonal prismatic coordination.[45] The structures of $La(OH)_3$,[45] other lanthanide trihydroxides (Ce,[46] Sm,[45] Gd,[45] Nd,[47] Ho,[45] and Er[45]), and $Y(OH)_3$[45] were determined by single-crystal X-ray diffraction methods; by neutron powder diffraction, the structures of $La(OH)_3$[48] and $Tb(OH)_3$ were determined.[49] The structure of $Nd(OH)_3$[47] was also studied by X-ray powder diffraction. The most common coordination numbers of the lanthanide ions are 8 and 9.

Four-coordinate tetrahedral La^{3+} (site IV in crystal 2) has been seen before. Four-coordinate tetrahedral Ln^{3+} (lanthanide) and Y^{3+} have been reported in $M[N(SiMe_3)_2]_3OPPh_3$ (M = La, Lu, and Eu),[50,51] in $[Lu(mesityl)_4]^-$,[50] and in $[Y(CH_2SiMe_3)_4]^-$.[50]

The coordination geometry of the seven-coordinate La^{3+} ions at site II in crystal 3, trigonally capped trigonal-prismatic, has not previously been reported for any cation. See Figure 16. Many examples of tetragonally capped trigonal-prismatic geometry, consistent with VSEPR theory, have been found.[30,31,52,53] The water molecules at W(1) have rotated 60° about the 3-fold axis from octahedral to trigonal prismatic positions with respect to the framework oxygens at O(2), perhaps in part because of the bridging water molecules at W(2). Least-squares refinement

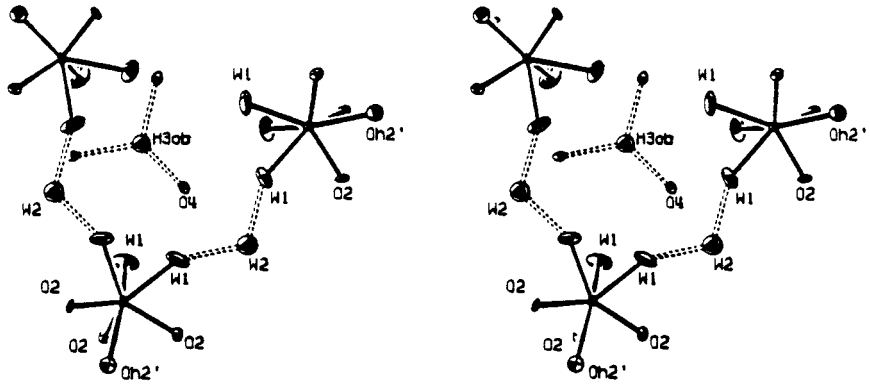

Figure 16. Stereoview of the supercage in crystal 3. The seven-coordinate atoms are La(II), and their coordination geometry is trigonally distorted trigonally capped trigonal prismatic. Each supercage has three La^{3+} ions at site II and 19 water molecules (only 11 are shown). Each La^{3+} ion coordinates to three water molecules, W(1). Water molecules at W(2) bridge between W(1) molecules. Eight other water molecules (not shown), three at W(3), three at W(4), and two at W(5) hydrogen bond to O(1) framework oxygens. W(3) and W(4) can also hydrogen bond to W(2). A hydronium ion, $H_3O(B)$ at site II, hydrogen bonds to three O(4) framework oxygens. Ellipsoids of 50% probability are shown.

gives about 10(2) water molecules at W(2); eight would allow two-thirds of the La(II) ions to be trigonally capped trigonal-prismatic, and 16 (three esd's greater than 10) would allow them all to have that coordination. Figure 16 shows 16 W(2) molecules per unit cell, two per supercage.

Although trigonally capped trigonal-prismatic coordination had not been seen before, a classic attempt to force this geometry by using a heptadentate chelating ligand was reported.[54] In $[M(py_3tren)]^{2+}$, where M(II) = Mn, Fe, Co, Ni, Cu, and Zn and $(py_3tren) = N\{CH_2CH_2N{=}C(H)(C_5H_4N)\}_3$, the coordination polyhedra of the six nitrogens (ignoring the trigonally capping seventh ligand (the tertiary amine)) are best described as trigonal antiprisms (TAP) (distorted octahedra) that are considerably distorted toward trigonal prismatic (TP). The capping nitrogen is so distant that it may be considered only weakly bonding, nearly noncoordinating.

In crystal 2, half of the sodalite units contain complete $La_4(OH)_4^{8+}$ "cubes" (distorted interpenetrating tetrahedra), and the other half contain $La_3(OH)(OH_2)_3^{8+}$ units. Yeom et al.[55] observed neutral Pb_4O_4 "cubes," less tetrahedrally distorted than those of La_4O_4 found in this work, in the sodalite units of zeolite X. Similarly, Ronay et al.[56] found $[(Pb^{2+})_3(O^{2-})(OH^-)_3]^{1+}$ clusters within the sodalite units of zeolite A; these are distorted Pb_4O_4 "cubes" with one corner (a Pb^{2+} ion) missing.

In $La(OH)_3$, whose structure was determined by Beall et al.[45] by single-crystal diffraction methods, the La−O bonds range from 2.551(3) to 2.588(3) Å, and the closest oxygen−oxygen distances range from 2.900(6) to 3.033(5) Å. The La(I′)−O(3) distances observed in crystals 1 and 2 are 2.524(12) and 2.538(17) Å, longer than the sum of the ionic radii of La^{3+} and O^{2-} (1.061 + 1.32 = 2.381),[38] but similar to Beall's distances. The La(I′)−O(6) distances in crystals 1 and 2 are 2.528(7) and 2.517(10) Å and the La(V)−O(5) distances are 2.48(6) and 2.46(12) Å, respectively, also similar to Beall's values. The O−O distances observed in crystals 1, 2, and 3 are all similar to Beall's.

It is clear that the zeolite framework was only somewhat harmed by ion exchange (crystal 3). The space group remained $Fd\bar{3}$ and the Si and Al positions are only partly compromised; the mean Al−O bond length should be 0.10−0.11 Å greater than the mean Si−O length,[27,57] but it is only 0.04 Å greater in crystal 3 (see Table 4). However, dehydration (crystals 1 and 2), even only partial dehydration at 22 °C, has caused some crystal damage as indicated by the change of space group to $Fd\bar{3}m$, indicating the loss of long-range Si and Al order. Bae et al.[58] observed this in Zn−X. The space group changed (and dealumination was observed), but only during the (high-temperature) vacuum dehydration process, not during ion exchange at 80 °C; this was confirmed by solid-state NMR of LSX powder.[59,60]

TABLE 4: Selected Interatomic Distances (Å) and Angles (deg)[a] for Crystal 3

Si−O(1)	1.660(9)	Al−O(1)	1.694(9)
Si−O(2)	1.659(9)	Al−O(2)	1.678(9)
Si−O(3)	1.620(9)	Al−O(3)	1.679(10)
Si−O(4)	1.645(9)	Al−O(4)	1.698(9)
mean Si−O	**1.646**	**mean Al−O**	**1.687**
O(1)−Si−O(2)	110.0(5)	O(1)−Al−O(2)	110.4(5)
O(1)−Si−O(3)	110.0(5)	O(1)−Al−O(3)	110.7(5)
O(1)−Si−O(4)	109.6(5)	O(1)−Al−O(4)	109.6(5)
O(2)−Si−O(3)	109.6(5)	O(2)−Al−O(3)	111.1(5)
O(2)−Si−O(4)	103.4(5)	O(2)−Al−O(4)	102.2(5)
O(3)−Si−O(4)	112.9(5)	O(3)−Al−O(4)	112.6(5)
Si−O(1)−Al	131.7(6)	Si−O(3)−Al	152.3(7)
Si−O(2)−Al	154.5(6)	Si−O(4)−Al	141.9(6)
La(I′)−O(2)	3.146(10)		
La(I′)−O(3)	2.776(12)		
La(I′)−OH2′	2.787(16)	O(3)−La(I′)−O(3)	98.3(5)
OH2′−H3O(A)	2.78(5)	OH2′−La(I′)−OH2′	87.0(3)
OH2′−O(2)	2.868(15)	OH2′−H3O(A)−OH2	126.2(12)
H3O(A)−La(I′)	3.28(7)	O(2)−OH2′−O(2)	92.9(6)
La(II)−OH2′	2.559(24)	O(2)−La(II)−O(2)	106.5(2)
La(II)−O(2)	2.591(8)	W(1)−La(II)−W(1)	69.7(6)
La(II)−O(4)	2.735(9)	W(1)−W(2)−W(1)	115(4)
La(II)−W(1)	2.608(15)	W(4)−W(2)−W(1)	107(5)
H3O(B)−O(4)	2.97(4)	W(1)−W(2)−W(3)	94(4)
W(1)−W(4)	2.80(5)		
W(1)−W(2)	2.67(17), 2.71(17)		
W(2)−W(4)	2.51(16)		
W(2)−W(3)	2.78(15)		
W(3)−O(1)	2.74(6)		
W(4)−O(1)	2.68(5)		
W(5)−O(1)	2.70(10)		

[a] The numbers in parentheses are the esd's in the units of the least significant digit given for the corresponding parameter.

Olson et al.[11] also found La^{3+} ions at sites I′, II, and V in hydrated $La_{33}Si_{104}Al_{88}O_{384}$, but his occupancies (12, 17, 4) are somewhat different, respectively, from those (8, 24, 1) found in this work. Nicely for this comparison, both structures have 33 La^{3+} ions per unit cell. Both structures indicate that the majority of the La^{3+} ions are in the supercages in hydrated La−X. It may be, if Olson had allowed his hydrated crystal to dry somewhat, perhaps by exposure to a low humidity atmosphere, that the La^{3+} ions had already begun their migration from site II in the supercage to site I′ in the sodalite unit. Simply

evacuating hydrated $La_{38}-X$ at 22 °C caused this process to go nearly to completion.

In $La_{30}-X$ dehydrated at 350 °C, all La^{3+} ions are found at site I′.[11] Compared to the current result for $La_{38}-X$ (crystal 1), this suggests that site I′ is filled before site V begins to fill when La−X is dehydrated. As in this work, Olson[11] found that the La^{3+} ions at site I′ each coordinate to three framework oxygens and to three μ_3-bridging nonframework oxygens; tetrahedrally distorted La_4O_4 cubes form in the sodalite units. In $La_{30}-X$,[11] the sodalite cavities are not quite full of these cubes because there are two too few La^{3+} ions per unit cell; also, the oxide ions at site I which complete the La_2O_3 continuum were not reported in $La_{30}-X$.[11]

Dehydration or steaming at elevated temperatures causes La^{3+} ions to move to I′ sites in zeolite Y also. Scherzer et al.,[14] after treatment at 540 °C, found that all La^{3+} ions occupy I′ sites at lower levels of La^{3+} exchange; in 98% exchanged La−Y, only 75% were at site I′ with 25% at site II. Nery et al.[15] also reported this movement to site I′ after treatment at 500 °C.

As discussed in the Introduction, Bennett and Smith found that most La^{3+} ions in zeolite X occupy site I after dehydration at various temperatures from ambient to 450 °C and that sites I′ and II are sparsely occupied.[12,13] Their results are entirely unlike those found in this and other previous work.[11,14,15]

Acknowledgment. We are grateful to David H. Olson for his encouragement of this work.

Supporting Information Available: Tables of observed and calculated structure factors squared with esd's. This material is available free of charge via the Internet at http://pubs.acs.org.

References and Notes

(1) Pickert, P. E.; Rabo, J. A.; Dempsey, E.; Schomaker, V. *Proceedings of the 3rd International Congress on Catalysis*; Amsterdam, 1964; p 714.
(2) Ruthven, D. M.; Kaul, B. K. *Ind. Eng. Chem. Res.* **1996**, *35*, 2060−2064.
(3) Venuto, P. B.; Hamilton, L. A.; Landis, P. S.; Wise, J. J. *J. Catal*. **1966**, *5*, 81−98.
(4) Choudary, B. M.; Matusek, K.; Bogyay, I.; Guczi, L. *J. Catal*. **1990**, *122*, 320−329.
(5) *Van Nostrand's Scientific Encyclopedia*, 8th ed.; Considine, D. M., Ed.; Van Nostrand Reinhold: New York, 1995; p 1838.
(6) Wegh, R. T.; Meijerink, A. *Chem. Phys. Lett.* **1995**, *246*, 495−498.
(7) Norby, T.; Dyrlie, O.; Kofstad, P. *Solid State Ionics* **1992**, *53*−*56*, 446−452.
(8) Chadwick, A. V.; Kennedy, K. M.; Morrison, G. *Ber. Bunsen-Ges. Phys. Chem.* **1997**, *101*, 1381−1385.
(9) Milne, S. J.; Brook, R. J.; Zhen, Y. S. *Br. Ceram. Proc.* **1989**, *41*, 243.
(10) Kalenck, Z.; Wolf, E. E. *Catal. Today* **1992**, *13*, 255.
(11) Olson, D. H.; Kokotailo, G. T.; Charnell, J. F. *J. Colloid. Interface Sci.* **1968**, *28*, 305−314.
(12) Bennett, J. M.; Smith, J. V. *Mater. Res. Bull.* **1968**, *3*, 865−875.
(13) Bennett, J. M.; Smith, J. V. *Mater. Res. Bull*. **1969**, *4*, 7−14.
(14) Scherzer, J.; Bass, J. L.; Hunter, F. D. *J. Phys. Chem.* **1975**, *79*, 1194−1199.
(15) Nery, J. G.; Mascarenhas, Y. P.; Bonagamba, T. J.; Mello, N. C.; Aguiar, E. F. S. *Zeolites* **1997**, *18*, 44−49.
(16) Aguiar, E. F. S.; Valle, M. L. M.; Silva, M. P.; Silva, D. F. *Zeolites* **1995**, *15*, 620−623.
(17) Lee, E. F. T.; Rees, L. V. C. *Zeolites* **1987**, *7*, 143−147.
(18) Lee, E. F. T.; Rees, L. V. C. *Zeolites* **1987**, *7*, 446−450.
(19) Rabo, J. A.; Angell, C. L.; Kasai, P. H.; Schomaker, V. *Discuss. Faraday Soc*. **1966**, 328−349.
(20) Bogomolov, V. N.; Petranovskii, V. P. *Zeolites* **1986**, *6*, 418−419.
(21) Bae, D.; Seff, K. *Micro. Meso. Mater.*, submitted for publication.
(22) Loewenstein, W. *Am. Mineral*. **1954**, *39*, 92−96.
(23) Peterson, B. K. *J. Phys. Chem. B* **1999**, *103*, 3145−3150.
(24) Sheldrick, G. M. *SHELXL93, Program for the Refinement of Crystal Structures*; University of Göttingen: Germany, 1993.
(25) *International Tables for X-ray Crystallography*; Kynoch Press: Birmingham, England, 1974; Vol. IV, p 73.
(26) Haniffa, R. M.; Seff, K. *J. Phys. Chem. B* **1998**, *102*, 2688−2695.
(27) Olson, D. H. *Zeolites* **1995**, *15*, 439−443.
(28) Sun, T.; Seff, K.; Heo, N. H.; Petranovskii, V. P. *Science* **1993**, *259*, 495−497.
(29) Sun, T.; Seff, K. *J. Phys. Chem.* **1994**, *98*, 5768−5772.
(30) Mingos, D. M. P. *Essential Trends in Inorganic Chemistry*; Oxford University Press: New York, 1998; pp 309−312.
(31) Rodgers, G. E. *Introduction to Coordination, Solid State, and Descriptive Inorganic Chemistry*; WCB/McGraw-Hill: New York, 1994; pp 44−47.
(32) Zalkin, A.; Templeton, D. H.; Karraker, D. G. *Inorg. Chem*. **1969**, *8*, 2680−2685.
(33) Narducci, A. A.; Ibers, J. A. *Inorg. Chem*. **1998**, *37*, 3798−3801.
(34) Wells, A. F. *Structural Inorganic Chemistry*, 5th ed.; Clarendon Press: Oxford, 1984; pp 543−547.
(35) Greis, O. *J. Solid State Chem*. **1980**, *34*, 39−44.
(36) Barnighausen, H.; Schiller, G. *J. Less-Common Metals* **1985**, *110*, 385−390.
(37) Wolf, R.; Hoppe, R. *Z. Anorg. Allg. Chem*. **1985**, *529*, 61−64.
(38) *Handbook of Chemistry and Physics*, 72nd ed.; Lide, D. R., Ed.; The Chemical Rubber Co.: Cleveland, OH, 1991/1992; 12-8.
(39) Kim, Y. Private communication.
(40) Zhu, L.; Seff, K. Unpublished work.
(41) Faucher, M.; Pannetier, J.; Charreire, Y.; Caro, P. *Acta Crystallogr., Sect. B* **1982**, *38*, 344−346.
(42) Fitch, A. N.; Jobic, H.; Renouprez, A. *J. Phys. Chem*. **1986**, *90*, 1311−1318.
(43) Yeom, Y. H.; Kim, A. N.; Kim, Y.; Song, S. H.; Seff, K. *J. Phys. Chem. B* **1998**, *102*, 6071−6077.
(44) Kim, Y.; Kim, A. N.; Han, Y. W.; Seff, K. *Proceedings of the 12th International Zeolite Conference*; Materials Research Society: Warrendale, PA, 1999; Vol. IV, pp 2839−2846.
(45) Beall, G. W.; Milligan, W. O.; Wolcott, H. A. *J. Inorg. Nucl. Chem*. **1977**, *39*, 65−70.
(46) Mullica, D. F.; Oliver, J. D.; Milligan, W. O. *Acta Crystallogr., Sect. B* **1979**, *35*, 2668−2670.
(47) Beall, G. W.; Milligan, W. O.; Dillin, D. R.; Williams, R. J.; McCoy, J. J. *Acta Crystallogr., Sect. B* **1976**, *32*, 2227−2229.
(48) Atoji, M.; Williams, D. E. *J. Chem. Phys*. **1959**, *31*, 329−331.
(49) Beall, G. W.; Milligan, W. O.; Korp, J.; Bernal, I. *Acta Crystallogr., Sect. B* **1977**, *33*, 3134−3136.
(50) Cotton, F. A.; Wilkinson, G. *Advanced Inorganic Chemistry*, 5th ed.; Wiley: New York, 1988, pp 959−961.
(51) Bradley, D. C.; Ghotra, J. S.; Hart, F. A.; Hursthouse, M. B.; Raithby, P. R. *J. Chem. Soc., Dalton Trans*. **1977**, 1166−1172.
(52) Gillespie, R. J.; Hargattai, I. *The VSEPR Model of Molecular Geometry*; Allyn and Bacon, Simon & Schuster, Inc.: Boston, 1991; p 190.
(53) Lin, Z.; Bytheway, I. *Inorg. Chem*. **1996**, *35*, 594−603.
(54) Kirchner, R. M.; Mealli, C.; Bailey, M.; Howe, N.; Torree, L. P.; Wilson, L. J.; Andrews, L. C.;Rose, N. J.; Lingafelter, E. C. *Coord. Chem. Rev*. **1987**, *77*, 89−163.
(55) Yeom, Y. H.; Kim, Y.; Seff, K. *J. Phys. Chem. B* **1997**, *101*, 5314−5318.
(56) Ronay, C.; Seff, K. *Zeolites* **1993**, *13*, 97−101.
(57) Yeom, Y. H.; Jang, S. B.; Kim, Y.; Song, S. H.; Seff, K. *J. Phys. Chem. B* **1997**, *101*, 6914−6920.
(58) Bae, D.; Zhen, S.; Seff, K. *J. Phys. Chem. B* **1999**, *103*, 5631−5636.
(59) Ciraolo, M. F.; Norby, P.; Hanson, J. C.; Corbin, D. R.; Grey, C. P. *J. Phys. Chem. B* **1999**, *103*, 346−356.
(60) Ciraolo, M. F.; Grey, C. P. Private communication.